SPECTROSCOPIC PROPERTIES OF $ZnPc(COOH)_4/Ch/Fe_3O_4$ SUPRAMOLECULAR ARCHITECTURES

PROPRIETĂȚI SPECTROSCOPICE ALE ARHITECTURURILOR SUPRAMOLECULARE $ZnPc(COOH)_4/Ch/Fe_3O_4$

CZU: 543.42:547.1 **https://doi.org/10.59295/spd2024n.79**

Alexandrina DRUTA,
ORCID: 0009-0004-0330-3039
e-mail: alexandrinadruta@gmail.com
Moldova State University
Ion LUNGU,
ORCID: 0000-0002-7117-672X
e-mail: ionlungu.usm@gmail.com
Moldova State University
Ana POPUȘOI,
ORCID: 0000-0002-7718-4771
e-mail: popusoi.ana@gmail.com
Moldova State University
Tamara POTLOG,
ORCID: 0000-0003-1243-9371
e-mail: tpotlog@gmail.com
Moldova State University
Petru BULMAGA,
ORCID: 0000-0003-0141-4902
e-mail: pbulmaga@mail.ru
Moldova State University
Roman RUSNAC,
ORCID: 0000-0002-5713-5251
e-mail: romanrusnac8@gmail.com
Moldova State University

Summary. *This paper presents the synthesis of $ZnPc(COOH)_4/Ch/Fe_3O_4$ supramolecular architectures at various $ZnPc(COOH)_4$ and Ch/Fe_3O_4 concentrations explored in the synthesis process. Ch/Fe_3O_4 composite was prepared by a simple solution mixing-evaporation method. The validation of the synthesis was achieved through FTIR analysis and UV-Vis spectroscopy. FTIR of composite indicated an interaction between chitosan and Fe_3O_4 NPs. The chemical interaction of $ZnPc(COOH)_4$ with Ch/F_3O_4 composite is confirmed by the shift of the signal from ν(C=O)) of protonated COOH groups in the FTIR spectrum of $ZnPc(COOH)_4$, associated with spitting, to (ν_{sym}(COO)) and (ν_{asym}(COO)) that correspond to deprotonated carboxylic group. The absorption spectra of $ZnPc(COOH)_4$ revealed IR Q band with two subbands situated at 640 nm*

700 nm. Also, the effect of various ZnPc(COOH) and Ch/Fe_3O_4 concentrations on absorbance of ZnPc(COOH)$_4$/Ch/Fe_3O_4 supramolecular architecture is discussed.

***Keywords**: ZnPc(COOH)$_4$ derivative, Ch/Fe_3O_4 composite, adsorption, self-assembly method.*

INTRODUCTION

Currently, metal phthalocyanines (MPcs) and their derivatives are found wide application in fabrication of light-emitting diodes, solar cells, transistors, materials for electrochromic displays and mediums for optical information registration [1-5]. The features of the molecular structure of MPcs make it possible to use them as catalysts and photocatalysts in different reactions, as good systems to generate free radical and excited state species [6]. These compounds are chemically and thermally stable. MPcs attract the attention of researchers as models of various photophysical processes, as well as the basis of diagnostic, phototherapeutic and other medical products [7-10]. MPcs exhibit superior photoproperties that make them a surely attractive class of photosensitizers for photodynamic therapy of cancer. Thus, MPcs are an extensive class of macroheterocyclic compounds with great scientific interest and broad application in many areas of science and technology. The purpose of this paper is to obtain water-soluble tetracarboxy zinc phthalocyanines (ZnPc(COOH)$_4$) that conjugate to chitosan/Fe_3O_4 surface modified nanoparticles, studying their absorption properties. The self-association and hetero-association of the compounds using UV/Vis spectrophotometer is simple, fast and inexpensive compared to other methods. Investigations of self-association of Fe_3O_4/Ch NP and their hetero-association with ZnPc(COOH)$_4$ in aqueous solution are interesting from the pharmacological point of view, since self- and hetero- associates and competitive binding may influence the activity of drugs.

EXPERIMENTAL

In a 250 mL flask, 1.0 g of chitosan dissolved in 200 mL of 2% acetic acid was prepared. To this solution, 1 mL of 60% hydrogen peroxide (H_2O_2) was added to disrupt intramacromolecular and inter-chain hydrogen bonds, followed by stirring for 3 hours using a magnetic stirrer, at 60 °C. For the functionalization of Fe_3O_4 nanoparticles with chitosan, 40 mL of the resulting solution was taken and 100 mg of Fe_3O_4 nanoparticles were added. The mixture was stirred using a magnetic stirrer for 20 hours at a constant temperature of 60 °C. After completion of stirring, the solution was allowed to cool, then filtered to separate the nanoparticles from any impurities. The water-soluble ZnPc(COOH)$_4$ was synthesized following procedures described in the [11]. Zinc-tetracarboxy-phthalocyanine was obtained with a yield exceeding 82% using the melting method and basic hydrolysis. All reagents and solvents, purchased from Merck at commercial reagent grade, were used as received without further purification. To investigate the interaction between ZnPc(COOH)$_4$ and Ch/Fe_3O_4, experiments were conducted with varying amounts of both materials. Each experiment involved different quantities of ZnPc(COOH)$_4$ combined with Ch/Fe_3O_4 to as-

sess how changes in Ch/Fe_3O_4 concentration influenced the absorption properties of the $ZnPc(COOH)_4$/Ch/Fe_3O_4 supramolecular architectures.

Absorption registration was conducted using the Cary 300 UV-VIS spectrophotometer, which recorded spectra ranging from 200 to 800 nm. Fourier Transform Infrared (FTIR) transmission spectra were recorded using the Bruker ALPHA Platinum-ATR spectrophotometer to investigate chemical composition and bond dynamics. Spectra were recorded from 4000 to 400 cm^{-1} at a resolution of 4 cm^{-1}, averaging 24 scans for each measurement.

RESULTS AND DISCUSSION

FTIR analysis

The FTIR spectrum of Fe_3O_4 is shown in Fig. 1(a). In this spectrum, a prominent peak at 528 cm^{-1} is observed, which can be attributed to the stretching vibration mode associated with Fe-O bonds in the Fe_3O_4 nanoparticles. This vibration mode, which is a characteristic feature of Fe_3O_4, is notably shifted to 485 cm^{-1} in the FTIR spectra of Ch/Fe_3O_4 nanoparticles (NPs). This shift indicates some interaction or modification due to the presence of chitosan. The modifications in the main characteristic bands of chitosan in the FTIR spectrum of the Ch/Fe_3O_4 system further support the binding of chitosan to Fe_3O_4 NPs. Specifically, the stretching vibration of the C-O bond, initially at 1023 cm^{-1}, shifts to 1030 cm^{-1}. The bending vibration of the NH_2 group shifts from 1643 cm^{-1} to 1587 cm^{-1}. The stretching vibrations of the O-H and C-H bonds, initially at 3291 cm^{-1} and 2870 cm^{-1}, respectively, shift to 3222 cm^{-1} and 2913 cm^{-1}. These shifts indicate that the chitosan molecules are interacting with the Fe_3O_4 NPs, likely through various types of chemical bonds or interactions.

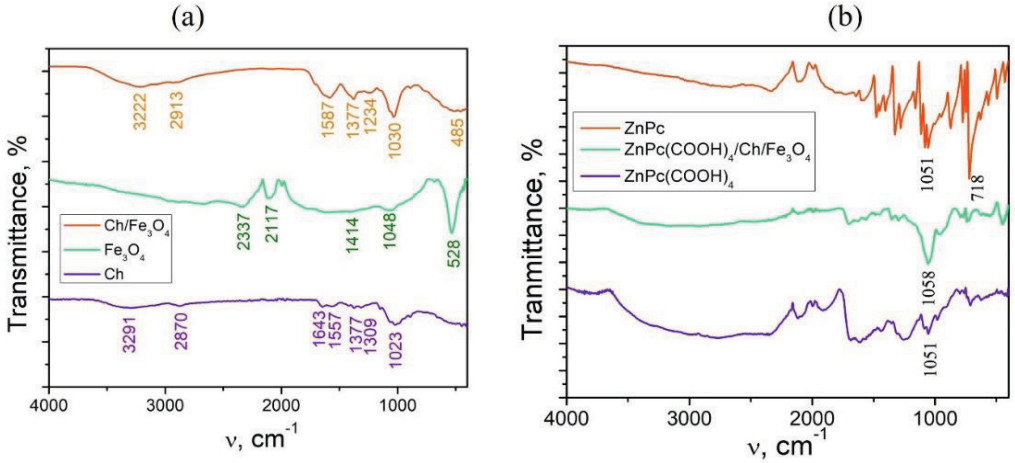


Figure 1. The FTIR spectra of Ch, Fe_3O_4, Ch/Fe_3O_4 NPs (a) and ZnPc, $ZnPc(COOH)_4$, $ZnPc(COOH)_4$/Ch/Fe_3O_4 (b)

The FTIR spectra of $ZnPc(COOH)_4$, presented in Fig. 1(b), show distinct bands that confirm the presence of specific functional groups. The band at 1703 cm^{-1} corresponds to

the characteristic stretching vibration of the carboxy group's carbonyl (C=O) bond. Another prominent band at 3455 cm^{-1} is associated with the hydroxyl (O-H) group. These bands confirm the successful formation of $ZnPc(COOH)_4$. Additionally, the FTIR spectra of $ZnPc(COOH)_4$ exhibit adsorption bands at 1093 cm^{-1} and within the 944–768 cm^{-1} region. These bands are attributed to the phthalocyanine ring skeleton, which is a key structural feature of $ZnPc(COOH)_4$. The presence of these bands further corroborates the formation and structure of the $ZnPc(COOH)_4$ compound.

UV-Vis spectroscopy,

The absorption spectra of $ZnPc(COOH)_4$ in DMSO/H_2O are presented in Fig. 2(a). The electronic absorption spectra are dominated by the broad Q band, which splits into two subbands at 640 nm and 700 nm. This splitting of the Q-bands can be attributed to the splitting of the LUMOs due to the substitution of electron-withdrawing groups and the expansion of the π system by the carboxy groups. Compared to the spectral data of unsubstituted ZnPc (675 nm) in DMSO, the Q-band of $ZnPc(COOH)_4$ is bathochromically shifted by at least 25 nm. As shown in Fig. 2(b), the absorbance of both subbands at 640 nm and 700 nm increase with the concentration of $ZnPc(COOH)_4$, indicating a linear relationship between absorbance and concentration (Fig. 2.b).

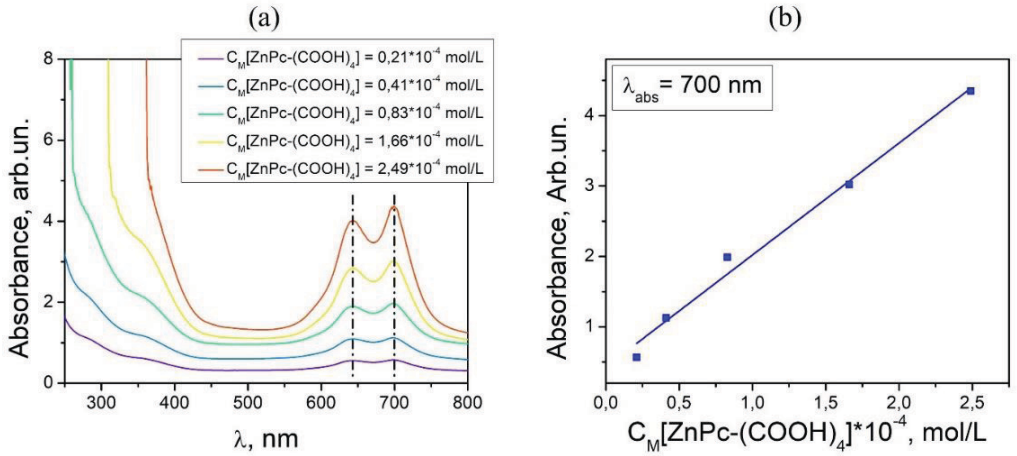


Figure 2. Absorption spectra of $ZnPc(COOH)_4$ in 1:1 ratio of DMSO/H_2O (a) and the calibration curve of absorbance versus concentration of $ZnPc(COOH)_4$ at λ_{abs} = 700 nm (b)

Figure 3(a) presents the UV-Vis spectra of chitosan (Ch), Fe_3O_4-NPs, and chitosan-coated Fe_3O_4 nanoparticles (Ch/Fe_3O_4-NPs). As shown, all three components exhibit absorption in the UV region. The Fe_3O_4 nanoparticles display a distinct maximum absorption peak at 280 nm, indicating strong UV absorption. The spectrum of pure chitosan also shows absorption in the UV region, but with different characteristics compared to the Fe_3O_4-NPs. The spectrum of chitosan had a single UV peak that is positioned at

280 nm. When Fe_3O_4 nanoparticles are coated with chitosan, forming the Ch/Fe_3O_4-NPs composite, the absorption spectrum combines features of both chitosan and Fe_3O_4 -NPs. This results in a modified absorption profile, demonstrating the presence and interaction of both components in the composite material.

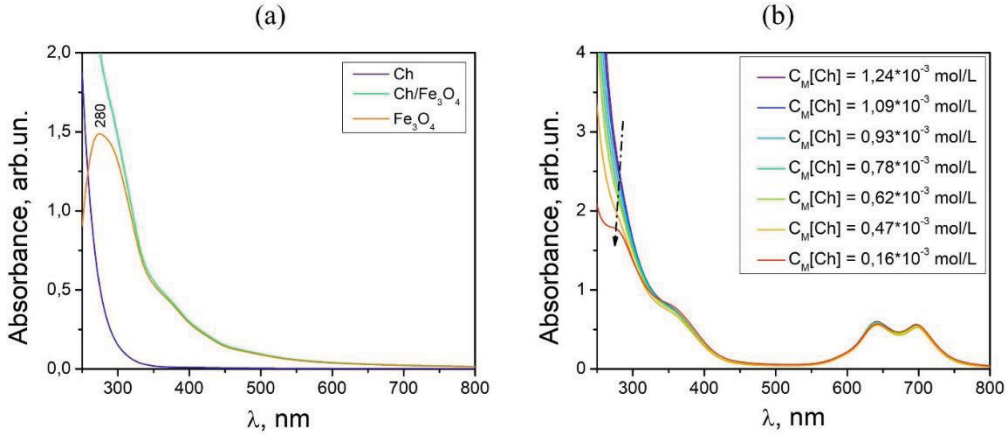


Figure 3. Absorption spectra of Ch, Fe_3O_4, Ch/Fe_3O_4 NPs (a) and ZnPc$(COOH)_4$/Ch/Fe_3O_4 in 1:1 ratio of DMSO/H_2O solvent (b)

Figure 3(b) presents the UV-Vis spectra of the ZnPc$(COOH)_4$/Ch compound, illustrating how the chitosan concentration, which varied from 0.16×10^{-3} mol/L to 1.24×10^{-3} mol/L, affects the absorption properties. As one can see, the concentration increase of chitosan significantly influences the UV absorption band of the compound, while Q band is not affected. Specifically, as the chitosan concentration increases, there is a noticeable enhancement in the UV absorbance peak situated at 280 nm. This enhancement can be attributed to the increased interaction and binding between the chitosan molecules and the ZnPc-$(COOH)_4$, leading to a more substantial self-assembly that exhibits stronger UV absorption.

Figure 4(a) presents UV-Vis spectra of the compound ZnPc$(COOH)_4$/Ch/Fe_3O_4 prepared by mechanical mixing. The concentration of Ch/Fe_3O_4 was varied from 0.27×10^{-3} mol/L to 2.16×10^{-3} mol/L, while the concentration of ZnPc$(COOH)_4$ remained constant at $C_{M[ZnPc\text{-}(COOH)_4]}=0.21 \times 10^{-4}$ mol/L. It is evident that increasing the concentration of Ch/Fe_3O_4 results in an overall increase in absorbance across the entire spectrum, leading to a higher baseline. Figure 4(b) shows UV-Vis spectra of the compound ZnPc$(COOH)_4$/Ch/Fe_3O_4, were the bond between the acetyl and nitrogen groups in Ch/Fe_3O_4 turns into an amine group (-NH_2) by adding acetic acid and H_2O_2 solution to Ch/Fe_3O_4 mixture. Here, the concentration of Ch/Fe_3O_4 was varied from 0.10×10^{-3} mol/L to 1.93×10^{-3} mol/L, with the concentration of ZnPc$(COOH)_4$ held constant at $C_{M[ZnPc\text{-}(COOH)_4]}=0.21 \times 10^{-4}$ mol/L. The Q band (600-800 nm) of ZnPc$(COOH)_4$ remains unaffected by varying Ch/Fe_3O_4 concentration. However, decreasing Ch/Fe_3O_4 concentration leads to reduced

absorption in the 250-450 nm region, particularly at the peak around 280 nm. This reduction indicates that Ch/Fe_3O_4 components play a crucial role in modifying ZnPc(COOH)$_4$ properties in Uv-Vis spectral domain, potentially forming complexes or aggregates with distinct electronic transitions. The highest UV adsorption capacity value is found in the composite with 1.93×10^{-3} mol/L Ch/Fe_3O_4 component.

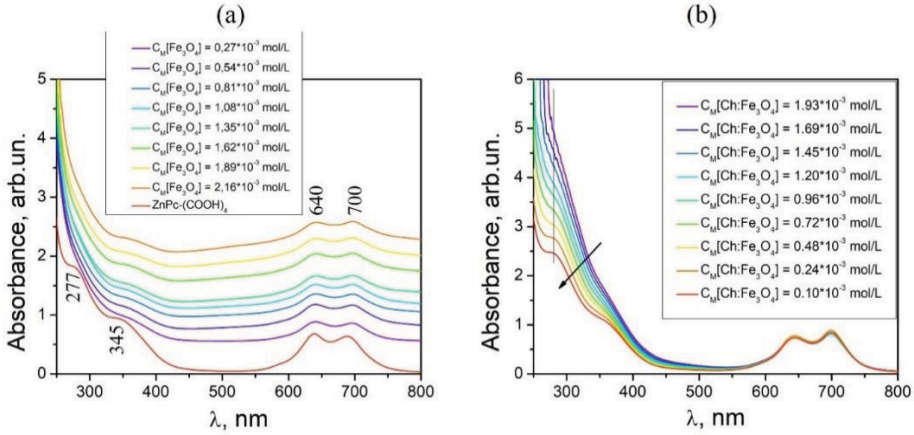


Figure 4. Absorption spectra of ZnPc(COOH)$_4$/Ch/Fe_3O_4 prepared by mechanical mixing (a) and through chemical bonding in 1:1 ratio of DMSO/H_2O solvent (b)

CONCLUSIONS

The modification and shift of the main characteristic FTIR bands, stretching C-O at 1021 cm^{-1}, bending NH_2 at 1648 cm^{-1}, stretching O-H (3300 cm^{-1}) and C-H (2864 cm^{-1-}) from chitosan in the IR spectrum of Ch/Fe_3O_4 system to 1073 and 1029 cm^{-1} (ν(C-O)), 1615 cm^{-1} (δ(NH_2)), 3431 cm^{-1} (ν(O-H)), 2935 and 2874 cm^{-1} (ν(C-H)) demonstrates the binding of chitosan to Fe_3O_4 nanoparticles. The absorption spectra of ZnPc(COOH)$_4$ revealed peak with maximum absorption in the IR region at 700 nm. ZnPc(COOH)$_4$/Ch/Fe_3O_4 supramolecular architecture produced from ZnPc(COOH)$_4$ derivative and Ch/Fe_3O_4 composite were manufactured by self-assembly in DMSO/H_2O solvent. The Q-band ZnPc(COOH)$_4$/Ch/Fe_3O_4 supramolecular architecture exhibited two peaks at λ_{max} = 640 nm and 700 nm and UV band at 280 nm, that changes to the variation of chitosan and Ch/Fe_3O_4 concentration due to the electrostatic interactions between NH_3^+ and COO^- bonds.

REFERENCES

1. WANG, H., LI, J. F., ZOU, M., SUI, T. Synthesis and transport property of AgSbTe2 as a promising thermoelectric compound. In: *Applied Physics Letters*, 2008, nr. 93(20), pp. 1-4.
2. SILVESTRI, F., LOPEZ-DUARTE, I., SEITZ, W., BEVERINA, L., MARTÍNEZ-DÍAZ, M. V., MARKS, T. J., TORRES, T. A squaraine–phthalocyanine

ensemble: towards molecular panchromatic sensitizers in solar cells. In: *Chemical communications*, 2009, nr. (30), pp. 4500-4502.

3. VAROTTO, A., NAM, C. Y., RADIVOJEVIC, I., PC TOMÉ, J., CAVALEIRO, J. A., BLACK, C. T., DRAIN, C. M. (2010). Phthalocyanine blends improve bulk heterojunction solar cells. In: *Journal of the American Chemical Society*, 2010, nr. 132(8), pp. 2552-2554.
4. ADEGOKE, O. O., INCE, M., MISHRA, A., GREEN, A., VARNAVSKI, O., MARTÍNEZ-DÍAZ, M. V., GOODSON III, T. Synthesis and ultrafast time resolved spectroscopy of peripherally functionalized zinc phthalocyanine bearing oligothienylene-ethynylene subunits. In: *The Journal of Physical Chemistry C*, 2013, nr. 117(40), pp. 20912-20918.
5. MISHRA, A., BÄUERLE, P. Niedermolekulare organische Halbleiter auf dem Vormarsch–Ausblick auf künftige Solartechniken. In: *Angewandte Chemie*, 2012, nr. 124(9), pp. 2060-2109.
6. ESCALONA HERNÁNDEZ, V., PADILLA-MARTÍNEZ, I. I., GARCÍA, R. A. V., RODRÍGUEZ, M. A. V., & HERNÁNDEZ-ORTIZ, O. J. Synthesis, and evaluation of photophysical properties of a potential DPP-derived photosensitizer for photodynamic therapy with DAD architecture. In: *Journal of Materials Science: Materials in Medicine*, 2024, nr. 35(1), pp. 11.
7. ASHOKKUMAR, R., KATHIRAVAN, A., RAMAMURTHY, P. Aggregation behaviour and electron injection/recombination dynamics of symmetrical and unsymmetrical Zn-phthalocyanines on TiO 2 film. In: *Physical Chemistry Chemical Physics*, 2014, nr. 16(3), pp. 1015-1021.
8. MORI, S., NAGATA, M., NAKAHATA, Y., YASUTA, K., GOTO, R., KIMURA, M., TAYA, M. Enhancement of incident photon-to-current conversion efficiency for phthalocyanine-sensitized solar cells by 3D molecular structuralization. In: *Journal of the American Chemical Society*, 2010, nr. 132(12), pp. 4054-4055.
9. GONZÁLEZ-RODRÍGUEZ, D., TORRES, T., GULDI, D. M., RIVERA, J., HERRANZ, M. Á., ECHEGOYEN, L. Subphthalocyanines: Tuneable molecular scaffolds for intramolecular electron and energy transfer processes. In: *Journal of the American Chemical Society*, 2004, nr. 126(20), pp. 6301-6313.
10. KIRBAÇ, E., ERDOĞMUŞ, A. New non-peripherally substituted zinc phthalocyanines; synthesis, and comparative photophysicochemical properties. In: *Journal of Molecular Structure*, 20220, nr. 1202, pp. 127392.
11. POTLOG, T., POPUSOI, A., LUNGU, I., ROBU, S., BULIMESTRU, I. Photophysics of tetracarboxy-zinc phthalocyanine photosensitizers. In: *RSC advances*, 2022, nr. 12(49), pp. 31778-31785.

Nota bene (N.B.): This research paper was financially supported by the Ministry of Education and Research of the Republic of Moldova, Moldova State University, subprogram “*Design of supramolecular architectures based on metal phthalocyanine derivatives – functionalized nanoparticles for medicine*”, #011209.